Collective directional memory controls the range of epithelial cell migration

Helena Canever[a,*], Hugo Lachuer[a,*], Quentin Delaunay[a], François Sipieter[a], Nicolas Audugé[a], Philippe P. Girard[a], and Nicolas Borghi[a]

[a]Université Paris-Cité, CNRS, Institut Jacques Monod, 75013 Paris, France
[*]These authors contributed equally

Cell migration is a fundamental behavior in multicellular development, regeneration, and homeostasis, which is deregulated in cancer. Epithelial cells migrate individually when isolated and collectively within a tissue. However, how interactions between cells affect their ability to explore space and their sensitivity to guidance signals is poorly understood. We show that isolated cells that are persistent random walkers adopt a superdiffusive behavior in an epithelium. The effect is stronger than external guidance cues and enables cells to reach greater distances than when isolated. This directional memory emerges from fractional Brownian motion that relies on velocity coordination between neighboring cells with intact intercellular adhesion. Furthermore, we show how the stability and mechanosensitivity of adhesion complexes ultimately regulate the speed of collective migration and the sensitivity to guidance signals via dimerization of the adhesion protein vinculin. Together, our results show how cell speed, persistence, and directionality define the efficiency of spatial cell exploration on short, intermediate, and long time scales, respectively.

Cell migration | Epithelium | Cell adhesion
Correspondence: ***nicolas.borghi@ijm.fr***

Introduction

In multicellular organisms, cell migration is an essential process in tissue morphogenesis, homeostasis, and repair. Deregulation of cell migration is also involved in the metastatic invasion of cancers (1). Cell migration occurs in different ways, depending on the intrinsic properties of cells and how they interact with each other and their environment. As a result, cells may migrate individually or collectively, guided by local or global signals (2).

For these reasons, how cells explore their environment and how cell interactions and guidance cues affect this exploration are fundamental questions that have motivated abundant research for over 70 years (3, 4). Since then, various models have proven useful in describing the exploration of space by individually migrating cells. Directional persistence has emerged as a consistent, though highly variable, feature depending on the type of cell or the context, and could arise from the non-Gaussian distribution of cell displacements, temporal velocity correlations, or both (5–8). When migrating collectively, neighbor cells typically exhibit correlated velocities that depend on their interactions (9–11). This coordination and the diverse mechanisms underlying it have been the subject of intense scrutiny for the past decade (12). In comparison, how each cell in the collective explores its environment has received much less attention, with a few exceptions (13–15). Remarkably, it remains unclear whether neighbor interactions actually help or hinder the exploratory capacity or sensitivity to guidance cues of each cell in the collective, much less whether and how they quantitatively or qualitatively affect the underlying cellular and molecular mechanisms of migration.

Adherent cells form Focal Adhesions (FAs) on their substrate, which they continuously assemble at their front and dissassemble at their back during migration (16). There, mechanosensory proteins, such as vinculin, provide force transmission from the contractile cytoskeleton (17). In cohesive tissues, cells also adhere to each other through cadherin-based Adherens Junctions (AJs) where α-catenin and vinculin enable dynamic connections with the cytoskeleton and force transmission (18). Vinculin comprises a head and a tail domain whose intramolecular interaction competes with intermolecular dimerization and binding to the actin cytoskeleton of its tail, and with binding of its head to adapter proteins in FAs and AJs (19). In AJs, α-catenin is this adapter, which also binds actin by its own tail (20). Vinculin deficiencies impact the migration of cells as individuals, in a collective, and with guidance cues, although in a cell type- and mutation-dependent manner (11, 21–32). Alpha-catenin deficiencies have an impact on guided and coordinated collective migration, involving the interaction of α-catenin with vinculin in AJs (11, 26, 33, 34). However, the lack of comparable metrics, scales and molecular, cellular and migratory contexts between studies makes it difficult for a general picture to emerge, where the functions of proteins in regulating the stability and mechanosensitivity of adhesions could explain how they control the intrinsic speed of cells, their persistence, and their responses to interactions with neighbors and guidance cues.

Here, we address this issue by comparing the exploratory ability of epithelial cells as individuals, in the collective and exposed to a guidance cue, while genetically disrupting the interactions of cells with their substrate and neighbors and monitoring the associated effects on the dynamics and mechanics of adhesion complexes. We show that individual epithelial cells migrate with transient directional memory and that vinculin regulates their speed by synergizing FA stability and cytoskeletal tension transmission through its dimerization and actin-binding abilities, respectively. In contrast, cells that migrate collectively acquire virtually infinite directional memory, which specifically requires α-catenin in AJs and re-

sults from the coordination of velocities between neighboring cells. In this context, vinculin additionally controls the speed of cells from their AJs through its impact on their mobility, but in a manner specifically dependent on its dimerization. Overall, this results in a spatial exploration that is less efficient than that of individual cells on time scales less than $\sim$ 3hrs but more efficient beyond that. Finally, cell guidance by an epithelial wound also requires α-catenin, but the directional bias is too small to significantly affect the efficiency of spatial exploration for hours. In this context of guided collective cell migration, vinculin dimerization further regulates cell speed from AJs by providing mechanosensitivity to the entire epithelium of the wound.

Results

Single epithelial cells are persistent random walkers. To characterize the motion of single epithelial cells, we tracked nucleus-stained MDCK cells overnight, sparsely plated on collagen-coated glass coverslips, which offer a reasonable approximation of the basement membrane(35–37) (see Materials and Methods)(Fig. 1A, movie 1). We found that a persistent random walk model (38, 39) was more likely than a pure or superdiffusion model to describe the average Mean Square Displacement (MSD) as function of time interval Δt: the MSD transitioned from ballistic (MSD $\sim \Delta t^2, \Delta t \to 0$) to pure diffusion (MSD $\sim \Delta t, \Delta t \to \infty$) with a persistence time of the order of 10min (Fig. 1B; Table S1). To confirm the underlying walk model, we examined the step size R for the time intervals $\Delta t = 10$min and $\Delta t = 3$hrs. In both cases, R followed a Rayleigh distribution, in agreement with a Gaussian walk regardless of temporal resolution (Fig. 1C, S1A). Finally, we examined the angular memory, which we define as the deviation of each elementary 10min step from the past direction over an increasingly longer past (Δt, see Materials and Methods). We found that its distribution was skewed towards small angles at small Δt and uniform at large Δt (Fig. S1B). In other words, the angular memory decreased with increasing Δt (Fig. 1D). Overall, these results show that single epithelial cells migrate as persistent random walkers, displaying transient directional persistence overcome by pure diffusion on longer time scales.

To investigate the robustness of this behavior, we examined the effects of overexpressing full-length (FL) vinculin or vinculin mutants, also equipped with a tension sensor module (40, 41). Specifically, we considered the T12 mutant with charge-to-alanine mutations in the tail that impair the head-tail interaction (42), the Y1065E (YE) mutant with a phosphomimetic mutation in the tail that impairs the tail-tail interaction (43) and the Tailless mutant (TL) lacking amino acids beyond 883 that are required for all tail interactions (44) (Fig. S2A). All constructs localized to FAs in stable cell lines (Fig. S2B,C), which exhibited an MSD better described by a persistent random walk model than by a pure or superdiffusion model (Fig. 2A, Table S1). The effects of mutant expression on persistence times and diffusion coefficients were variable and did not show a correlation (Fig. S2D). In addition, the diffusion coefficient scaled well with the squared apparent speed with a common persistence time for all cell lines (Fig. S2E), showing that cell lines differed primarily in apparent speed rather than persistence. Specifically, TL and YE mutants with impaired actin-tail or tail-tail interactions decreased cell speed, while the T12 mutant with altered head-tail interaction increased cell speed relative to FL vinculin (Fig. 2B). This could not be explained by differences in expression levels between cell lines since the effects of YE and TL were stronger than those of FL despite an equal or lower expression, and those of T12 completely opposite despite a higher expression (Fig. S2F). Rather, this indicated a dominant effect, consistent with previous reports (44). Overall, these results show that the persistence, but not the speed of single migrating cells is robust to mutations in the FA protein vinculin.

The combination of Focal Adhesion stability and force transmission from the cytoskeleton predicts the migration speed of single cells. The transmission of cytoskeletal forces through FAs is essentially based on vinculin (44–46). Thus, to identify the underlying cellular mechanisms and molecular determinants of speed regulation by FAs, we took advantage of the tension sensor module in vinculin and its mutants to assess their mechanical state by Molecular Tension Microscopy (Fig. 2C) (see Materials and Methods). We found that alteration of actin-tail and head-tail interactions (TL and T12) decreased and increased vinculin tension relative to FL vinculin, respectively (Fig. 2D), as seen in other cell types (40, 41). In contrast, alteration of the tail-tail interaction (YE) did not substantially affect vinculin tension, meaning that vinculin dimerization is unnecessary for force transmission (Fig. 2D). Next, we investigated a potential relationship between vinculin tension and single cell speed across mutants, but found no significant correlation (Fig. S2G), indicating that single cell speed is not simply a result of vinculin force transmission.

The stability of the core cytoskeletal linkers of FAs is based on vinculin (30, 47). Therefore, we investigated the effects of mutations on vinculin turnover by Fluorescence Recovery After Photobleaching (FRAP, Fig. S2H, movie 2) (see Materials and Methods). We found that TL and T12 mutants, both of which impair head-tail interaction, had a significantly higher immobile fraction than FL vinculin (Fig. 2E), consistent with previous studies in other cell types (30, 44, 47–50). This shows that impaired head-tail interaction, regardless of tension, is sufficient for vinculin stability. In contrast, the YE mutant that impairs the tail-tail interaction showed a significantly smaller immobile fraction (Fig. 2E). This shows that vinculin dimerization promotes its stability. Additionally, this shows that cell migration speed does not simply result from vinculin stability since T12 and TL induce opposite effects on migration speed while both stabilize vinculin, and T12 and YE have antagonist effects on vinculin stability while both promote cell speed.

Together, this supports that migration speed decreases upon loss of force transmission or FA stability (TL and YE) and increases upon strengthening of both (T12). We therefore propose that single cell migration speed is the product of FA sta-

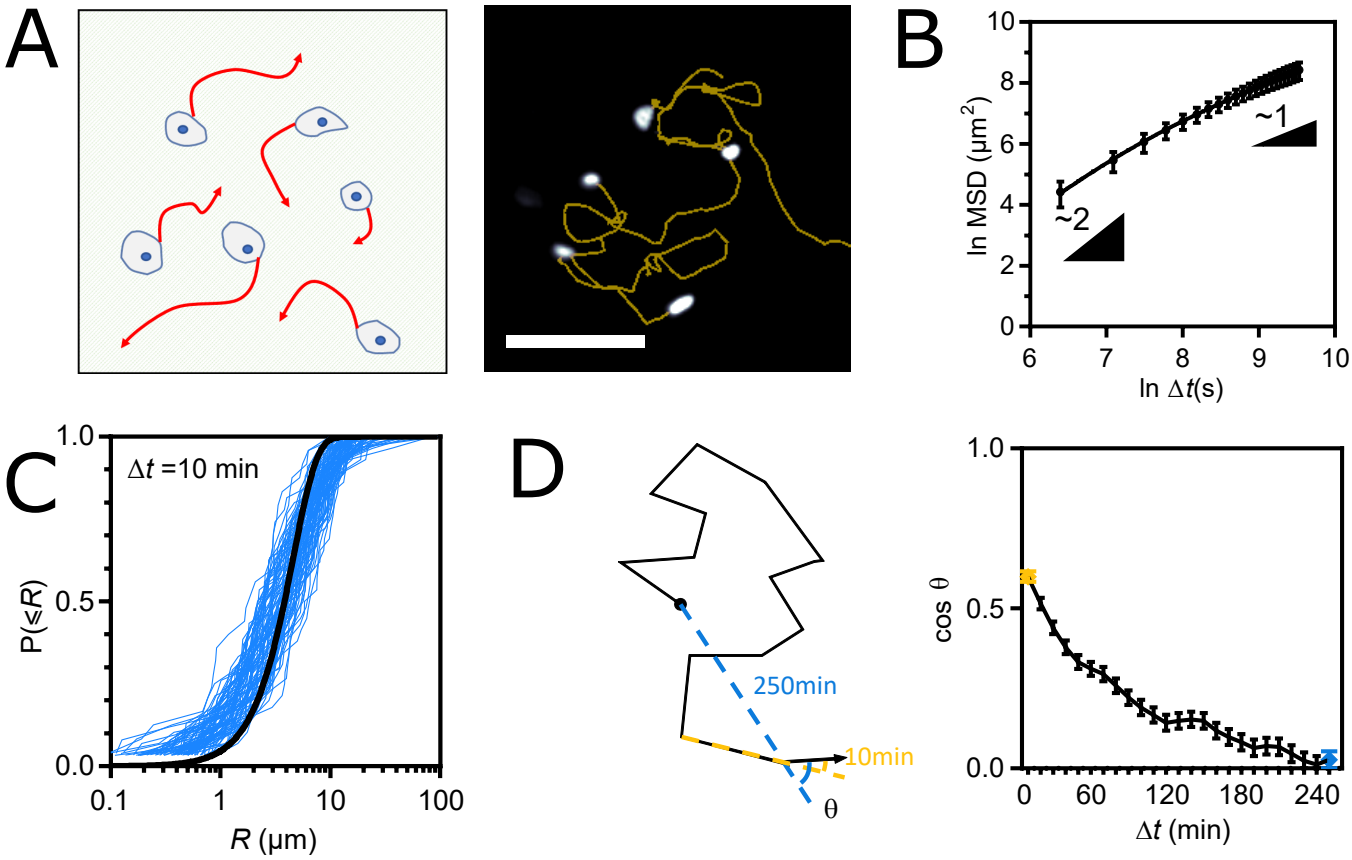

Fig. 1. (A) Left: Schematic representation of the single cell migration assay. Right: fluorescence image of nucleus-stained cells and their migration tracks in yellow. Scale bar = 100μm. (B) MSD(Δt) of WT cells fit with the Fürth model. (C) Cumulative distributions of the step length R for $\Delta t = 10$min. One blue curve per frame pair along a movie. The black line is a global fit of all blue curves with a cumulative Rayleigh distribution function. (D) Left: Schematic migration track and angular memory ($\cos\theta(\Delta t)$, see Materials and Methods) at $\Delta t = 10$min (yellow) and $\Delta t = 250$min (blue). Right: Angular memory ($\cos\theta(\Delta t)$) between $\Delta t = 10$min (yellow dot) and $\Delta t = 250$min (blue dot). Data of (B-D) from 94 cell tracks of 2 independent experiments. Mean $\pm$ SEM.

bility and force transmission, the former enabled by vinculin tail-tail interaction and the latter by vinculin-actin binding, and both competed for by its head-tail interaction (Fig.2F).

Collectively migrating epithelial cells are superdiffusive, fractional Brownian walkers. To assess how intercellular adhesion affects the persistent random walk of cells, we tracked MDCK cells plated at confluence on collagen-coated glass coverslips (see Materials and Methods) (Fig. 3A, movie 3). In these conditions, the cell shape index (~ 4.2) was well above the rigidity threshold ($q \simeq 3.8$, Fig. S3A) (see Materials and Methods), which supports that the tissue behaved as a fluid with negligible resistance arising from cortical tension against cell rearrangements (51). We found that within the same time frame as in single cell migration experiments, cells no longer migrated as persistent random walkers but adopted superdiffusive behavior with an anomalous exponent of approximately 1.7 (Fig. 3B, Table S2). Remarkably, this superdiffusive behavior allowed cells to eventually reach a greater distance than single cells in the same amount of time, even though confluence also lowered their apparent speed (Fig. S3B).

To distinguish between the various walk models that could produce such a superdiffusive behavior (Lévy flight, fractional Brownian motion, or their combinations (7, 52)), we examined the step size distributions and found that they were consistent with a Gaussian walk on any time scale up to $\Delta t = 3$hrs (Fig. 3C, S3C). However, we found that the angular deviation of any 10min-step from the direction of the previous step was skewed toward small angles and invariant with the time scale of the previous step up to $\Delta t = 250$min (Fig. S3D). In other words, the angular memory never disappeared within our experimental time frame, unlike that of single cells (Fig. 3D compared to Fig. 1D). Gaussianity and virtually infinite directional memory are characteristics of a pure fractional Brownian motion and thus rule out Lévy walks or other combination. Cell superdiffusion thus emerges from a fractional Brownian motion.

The transition in directional memory emerges from Adherens Junction-mediated intercellular adhesion. To assess whether these effects resulted from simple steric hindrance due to crowding by neighboring cells or from genuine AJ-mediated intercellular adhesion, we examined the collective migration of cells depleted of α-catenin, without which cells cannot form AJs (53) (see Materials and Methods). Remarkably, the cells lost most of their superdiffusive behavior (with an anomalous exponent α dropping from 1.7 to ~ 1.2) and recovered a higher cell speed, despite being as crowded as WT cells (Fig. 3E). Consistently, angular mem-

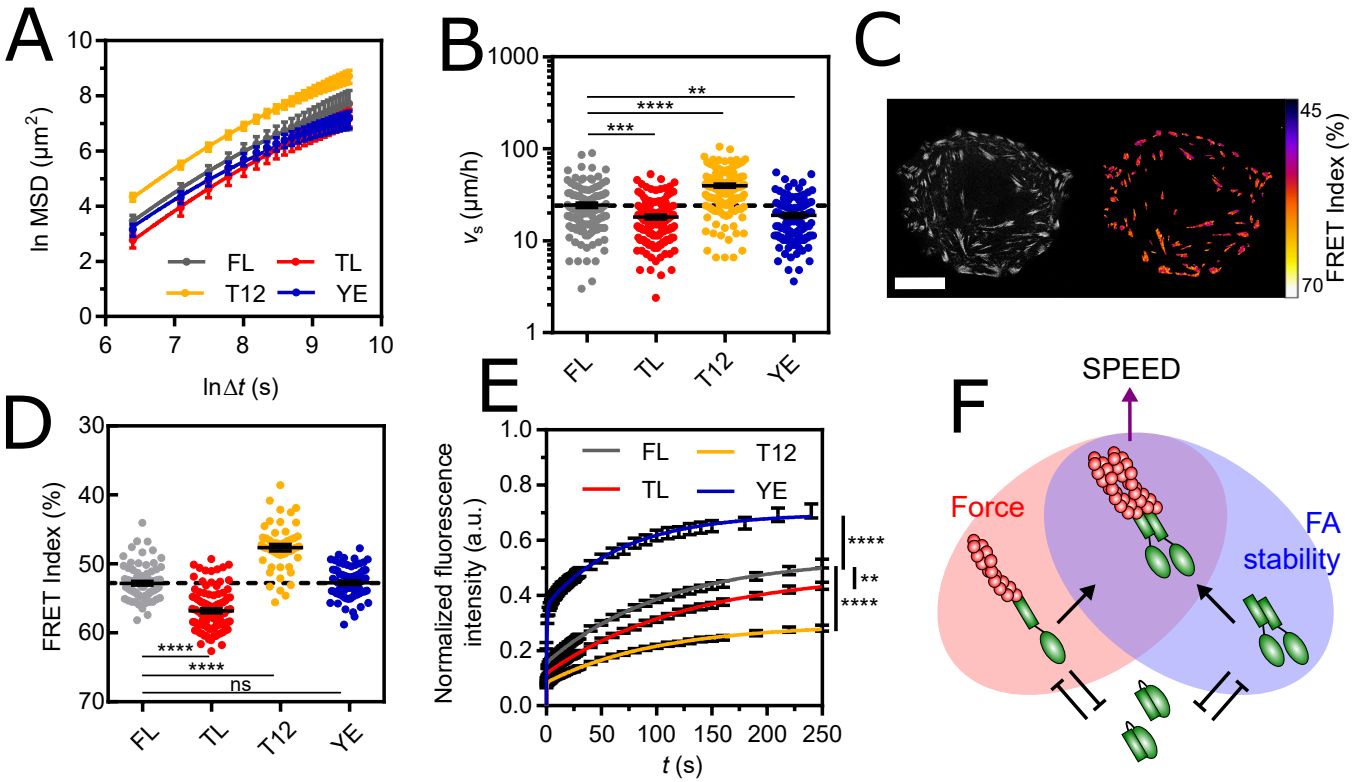

Fig. 2. (A) MSD(Δt) of vinculin FL and mutant cells fit with the Fürth model. (B) Apparent speed of single, vinculin FL and mutant cells. (C) Left: direct fluorescence of vinculin TSMod in a single cell. Right: FRET Index map (see Materials and Methods). Scale bar = 20 μm. (D) FRET Index of TSMod in the FL, TL, T12 and YE constructs in FAs. (E) Fluorescence recovery after photobleaching of FL, TL, T12 and YE constructs in FAs fit with a 2-phases association model. (F) Proposed model: at FAs, the head-tail interaction of vinculin (green) competes with both tail dimerization and actin filaments (red) binding, which provide FA stability and force transmission, respectively, together promoting cell speed. Data of (A,B) from 125 (FL), 129 (TL), 193 (T12) and 110 (YE) cell tracks of 3 independent experiments. Data of (D) from 81 (FL), 102 (TL), 52 (T12) and 84 (YE) cells of 4 (FL) and 3 (TL, T12, YE) independent experiments. Data of (E) from 105 (FL), 112 (TL), 118 (T12) and 65 (YE) cells of 2 independent experiments. Mean $\pm$ SEM. Two-tailed Mann-Whitney tests between each mutant and FL (B,D). Extra-sum-of-squares F test with shared immobile fraction between each mutant and FL as the null hypothesis (E).

ory vanished in the experimental time frame (Fig. 3F), as for single migrating cells. Next, to test whether cadherin subtypes could compensate for each other, we used cells depleted of E-cadherin but that retained cadherin-6 expression (53) (see Materials and Methods). These cells exhibited a slightly higher anomalous exponent than WT cells (Fig. 3E) and, consistently, infinite angular memory (Fig. 3F). This shows that E-cadherin specifically is largely dispensable, if not slightly detrimental, for cells to migrate in a superdiffusive manner, just as it is for the maintenance of AJs (53). Similarly, different cadherin subtypes can compensate for the defficiency of E-cadherin in other contexts (54–56).
Therefore, the drop in cell speed and the transition in directional memory observed at confluence are the results of *bona fide* AJ-mediated intercellular adhesion, but independently of the cadherin subtype.

Velocity coordination between neighbors suffices to produce superdiffusion. Because velocity coordination is lost upon disruption of AJs by α-catenin depletion (Fig. S3E) (11), we sought to determine whether this effect of intercellular adhesion sufficed to confer a superdiffusive behavior to confluent cells regardless of other intercelullar adhesion features. To do so, we turned to *in silico* simulations of interacting self-propelled particles (SPP, see Materials and Methods). First, we modeled individual cells as persistent random walkers with the same apparent speed and intrinsic persistence P_0 in isolation for all cells, in compliance with single cell migration results. Accordingly, P_0 is directly proportional to the time τ needed to make a step and a function of the intrinsic directional freedom of the cell between each step. Then, we modeled velocity coordination with a classic Vicsek interaction within a cell-scale distance d (57), and explored the MSD of particles at densities ρ covering isolated cells up to beyond confluence. We found that as the number of interacting neighbors $n = \pi\rho d^2$ increased, the effective persistence P of the particles increasingly diverged from P_0 before the migration behavior transitioned to superdiffusion (Fig. 3G). Strikingly, for a range of realistic values of interaction distance $d \sim 10 - 30\mu$m, confluent density $\rho \sim 2000 - 4000$ cells/mm^2 and various degrees of directional freedom affecting $1 \lessapprox P_0/\tau \lessapprox 10$, the anomalous exponent fell around $\alpha \sim 1.7$ (yellow region), consistent with experimental observations (see Fig. 3).

Furthermore, this model predicted that provided a minimal number of interacting neighbors was reached, persistent random walkers would always transition to superdiffusers regardless of their intrinsic persistence. To test this, we tracked the single and collective cell migration of RPE-1 cells, another epithelial cell line (Fig. S3F, movies 4, 5). We found that single RPE-1 cell migration was also much better de-

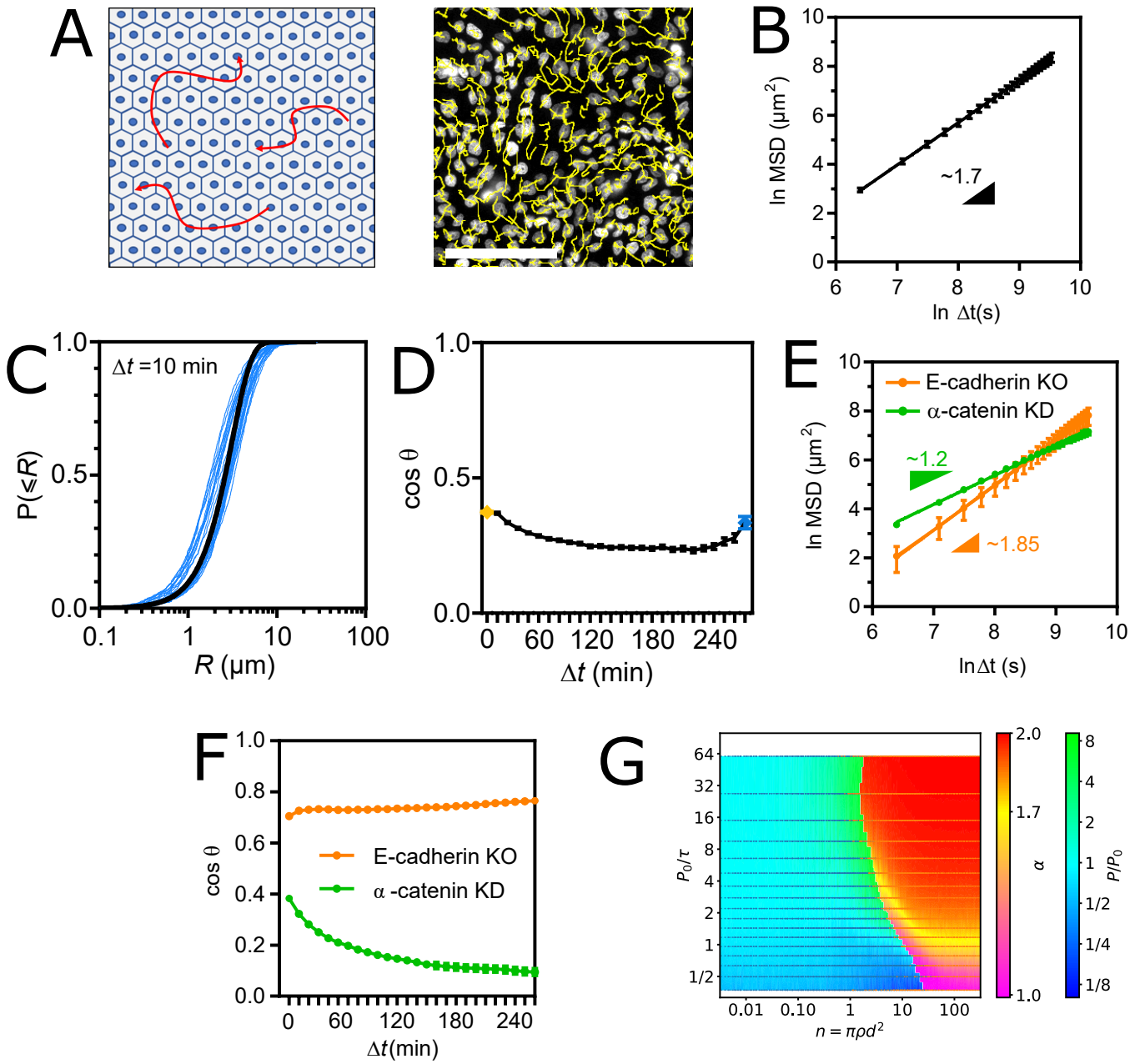

Fig. 3. (A) Left: Schematic representation of the collective cell migration assay. Right: fluorescence image of nucleus-stained cells and their migration tracks in yellow. Scale bar = 100μm. (B) MSD(Δt) of WT cells fit with a straight line in ln-ln scale . (C) Cumulative distributions of the step length R for $\Delta t = 10$min. One blue curve per frame pair along a movie. The black line is a global fit of all blue curves with a cumulative Rayleigh distribution function. (D) Angular memory ($\cos\theta(\Delta t)$) between $\Delta t = 10$min (yellow dot) and $\Delta t = 250$min (blue dot). (E) MSD(Δt) of E-cadherin KO and α-catenin KD cells fit with a straight line in ln-ln scale. (F) Angular memory ($\cos\theta(\Delta t)$) of E-cadherin KO and α-catenin KD cells. Data of (B-D) from 11 Fields Of View (FOV, 500-1000 tracks each) of 3 independent experiments. Data of (E-F) from 3 (E-cadherin KO) and 4 (α-catenin KD) FOV (500-100 tracks each) of 2 (E-cadherin KO) and 3 (α-catenin KD) independent experiments. Mean $\pm$ SEM. (G) Migration behavior of Self-Propelled Particles with Vicsek interactions as a function of P_0/τ and number of interacting neighbors $n = \pi\rho d^2$. Blue and orange points are simulation coordinates that resulted in persistent and super-diffusive behavior, respectively. Cold and warm color backgrounds are interpolations from points above of P/P_0 and α values, respectively.

scribed by a persistent random walk than by a diffusion model, although with a persistence around 1 hr, making the difference hard to notice by eye within the experimental time window (Fig. S3E). Moreover, RPE-1 cell migration at confluence was again much better described by a superdiffusion model with an anomalous exponent around 1.6, as expected (Fig. S3E).

We conclude that velocity coordination is a feature of intercellular adhesion that suffices to produce superdiffusion at confluence in a manner that is very robust to the intrinsic persistence of cells, as predicted by our model.

Stabilization of Adherens Junctions by vinculin dimerization lowers cell migration speed. To further investigate the regulation of collective migration by intercellular adhesions, we examined the effects of confluence on vinculin mutant cell lines. All cell lines behaved as fluid tissues and their cells remained superdiffusive regardless of the expressed mutant (Fig. S4A, Fig. 4A, Table S3), showing that vinculin plays little or no role in the regulation of directional

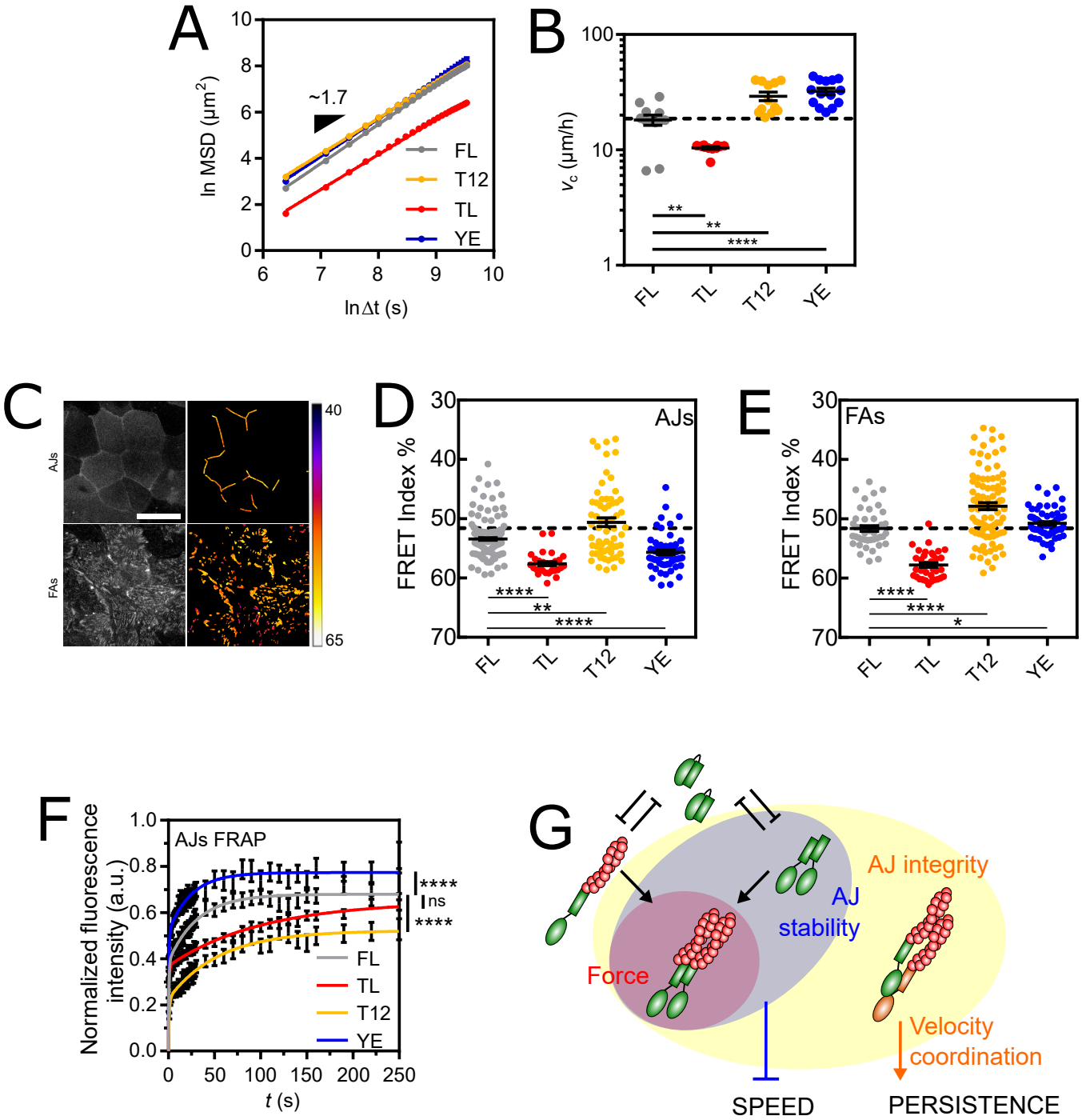

Fig. 4. (A) MSD(Δt) of vinculin FL and mutant cells fit with a straight line in ln-ln scale. (B) Apparent speed of vinculin FL and mutant cells at confluence. (C) Left: direct fluorescence of vinculin TSMod in a confluent monolayer. Right: FRET Index map (see Materials and Methods). Top: in the AJs plane. Bottom: in the FAs plane. Scale bar = 20μm. (D) FRET Index of TSMod in the FL, TL, T12 and YE constructs in AJs at confluence. (E) FRET Index of TSMod in the FL, TL, T12 and YE constructs in FAs at confluence. (F) Fluorescence recovery after photobleaching of FL, TL, T12 and YE constructs in AJs fit with a 2-phases association model. (G) Proposed model: at AJs, α-catenin (orange) provides AJ integrity (connection to the cytoskeleton), which promotes persistence. The head-tail interaction of vinculin (green) competes with both tail dimerization and actin filaments (red) binding. Dimerization provides AJ stability, which slows cell down. Data of (A-B) from 12 (FL), 11 (TL, T12) and 14 (YE) FOV (500-1000 tracks each) of 3 independent experiments. Data of (D) from 169 (FL), 30 (TL) and 64 (T12, YE) contacts of 5 (FL) and 3 (TL, T12, YE) independent experiments, and (E) from 45 (FL), 35 (TL), 104 (T12) and 67 (YE) cells of 4 (FL) and 3 (TL, T12, YE) independent experiments. Data of (F) from 75 (FL), 137 (TL), 78 (T12) and 36 (YE) contacts of 4 (FL, TL, T12) and 3 (YE) independent experiments. Mean $\pm$ SEM. Two-tailed Mann-Whitney tests between each mutant and FL (B,D,E). Extra-sum-of-squares F test with shared immobile fraction between each mutant and FL as the null hypothesis (F).

memory by intercellular adhesions.

Therefore, we examined cell speed. We reasoned that if vinculin neither plays a role in the regulation of cell speed by AJs, cell speed at confluence can be entirely predicted from single cell speed for each vinculin construct. We indeed found that TL and T12 mutants remained slower and faster, respectively, than FL (Fig. 4B). Moreover, the three cell lines exhibited the same $\sim 10\mu\mathrm{m/h}$ decrease in speed as WT cells at confluence compared to single cells (Fig. S4C). This indicates that AJs decrease cell speed independently of the effects of these mutants, which therefore have no other role in cell migration at confluence than those at FAs as in single cells. In contrast, the YE mutant was faster than FL at confluence (Fig. 4B), while it was slightly slower in single cells (see Fig. 2B). In fact, confluence induced a $\sim 10\mu\mathrm{m/h}$ increase, instead of a decrease in cell speed for this mutant (Fig. S4C). Altogether, this supports that functions impaired in YE, and not TL or T12, are key for the AJ-dependent decrease in cell speed at confluence.

At confluence, cortical actomyosin contractility promotes the recruitment and tension of vinculin in AJs (58). Here, all vinculin constructs colocalized with α-catenin and actin in intercellular contacts (Fig. S4D,E). To assess what distinguishes the YE mutant from the other constructs, we compared their relative recruitment and tension. In AJs, we found that YE showed a lower recruitment and tension than FL and T12, similar to TL, although to a milder extent (Fig. S4F, 4D). In FAs, in contrast, YE experienced a higher tension than FL, similar to T12, although to a milder extent (Fig. 4E). Altogether, the effect of YE on tension was neither different nor even stronger than that of the other mutants (Fig. S4G). Furthermore, there was no correlation between tension and cell migration speed among cell lines (Fig. S4H). This rules out tension as a regulator of collective cell migration speed.

Thus, we examined the stability of vinculin and its mutants by FRAP in AJs (Fig. S4I, movie 6), the stability of which is based on that of vinculin(18). FRAP experiments showed that the YE mutant had a significantly smaller immobile fraction than FL vinculin, while the TL and T12 mutants had larger immobile fractions, just as in FAs, although only that of the T12 mutant was significantly different (Fig. 4F). Therefore, the lack of stability in AJs is the unique difference between YE and the other mutants that appears at confluence. Overall, these results support that the stabilization of AJs (with TL, FL or T12), regardless of the tension they transmit through vinculin, equally lowers the speed of cell migration initially determined by FAs. In contrast, when AJs are unstable (YE), cells collectively migrate proportionally faster than single cells. Therefore, we propose that vinculin tail dimerization ensures the stability of AJs, which adapts the collective cell migration speed to the single cell migration speed (Fig. 4G).

Superdiffusion overcomes the weak directional bias caused by adhesion-dependent sensitivity to external guidance cues. While cells adopt a superdiffusive behavior at confluence, they do so in any possible direction. Thus, we sought to evaluate how the addition of an external guidance cue would affect the spatial exploration efficiency of collectively migrating cells. In principle, a directional bias eventually overcomes any diffusion behavior on a sufficiently long time scale, resulting in a ballistic motion (MSD $\sim \Delta t^2, \Delta t \to \infty$). To assess when it would occur, we wounded a confluent epithelial monolayer and tracked nucleus-stained cells as they invaded the free surface to close the wound (Fig. 5A, movie 7). Approximately 3 hours after wounding, the apparent speed of cells stabilized (Fig. S5A), consistent with previous reports (59), and was independent of the distance to the wound (Fig. S5B). Thus, we examined the MSD from 3hrs after wounding. Surprisingly, we found that the migration behavior remained superdiffusive with an anomalous exponent around 1.6 (Fig. 5B). Furthermore, as in the case of unbiased collective migration, the anomalous exponent decreased to around 1.2 for cells depleted of α-catenin, whereas cells depleted of E-cadherin remained superdiffusive, (Fig. 5C). Similarly, vinculin mutants did not affect superdiffusive behavior (Fig. 5D). Overall, these results show that space exploration efficiency remains dominated by the superdiffusive behavior of cells up to a few hours after exposure to an external guidance cue.

This raised the question whether cell velocity was biased at all or if cells merely filled the wounded area by isotropic superdiffusion. To assess this, we examined the angular distribution of cell velocities. In the steady state speed regime (at 6hrs), a directional bias was clearly visible (Fig. 5E). The bias appeared within 3hrs post-wound and remained stable throughout (Fig. 5F). This shows that a directional bias of such magnitude maintained from 3hrs onward is too weak to substantially improve the spatial reach of collectively migrating cells in the time range of the experiment. Finally, we asked whether disrupted AJs would alter the sensitivity of cells to directional bias. Remarkably, cells depleted of α-catenin exhibited very little directional bias compared to WT cells (Fig. 5F). Together, this shows that AJ-mediated intercellular adhesion is required not only for cells to acquire virtually infinite directional memory (see Fig. 3E, 5C), but also for them to perceive and migrate toward external guidance cues.

Vinculin dimerization scales wound healing rate to the collective cell migration speed through the regulation of Adherens Junction mechanosensitivity. Next, we wondered whether AJs were involved in the regulation of directed collective cell migration through additional mechanisms distinct from the regulation of directional memory (see Fig. 3E, 5C) and sensitivity to guidance cues by α-catenin (see Fig. 5F), and of speed by vinculin dimerization and stabilization of AJs at confluence (see Fig. S4C). To do so, we assessed whether the rate of wound healing, at which the wounded epithelium covers the free surface (see Materials and Methods), could be predicted from the speed of collective cell migration at confluence in vinculin mutant cell lines (see Fig. 4B). We expected a correlation if no additional regulation depended on vinculin. We found that this was mostly the case, with the exception of the YE mutant. Indeed, while vinculin FL, T12 and TL cells closed the wound at a rate pro-

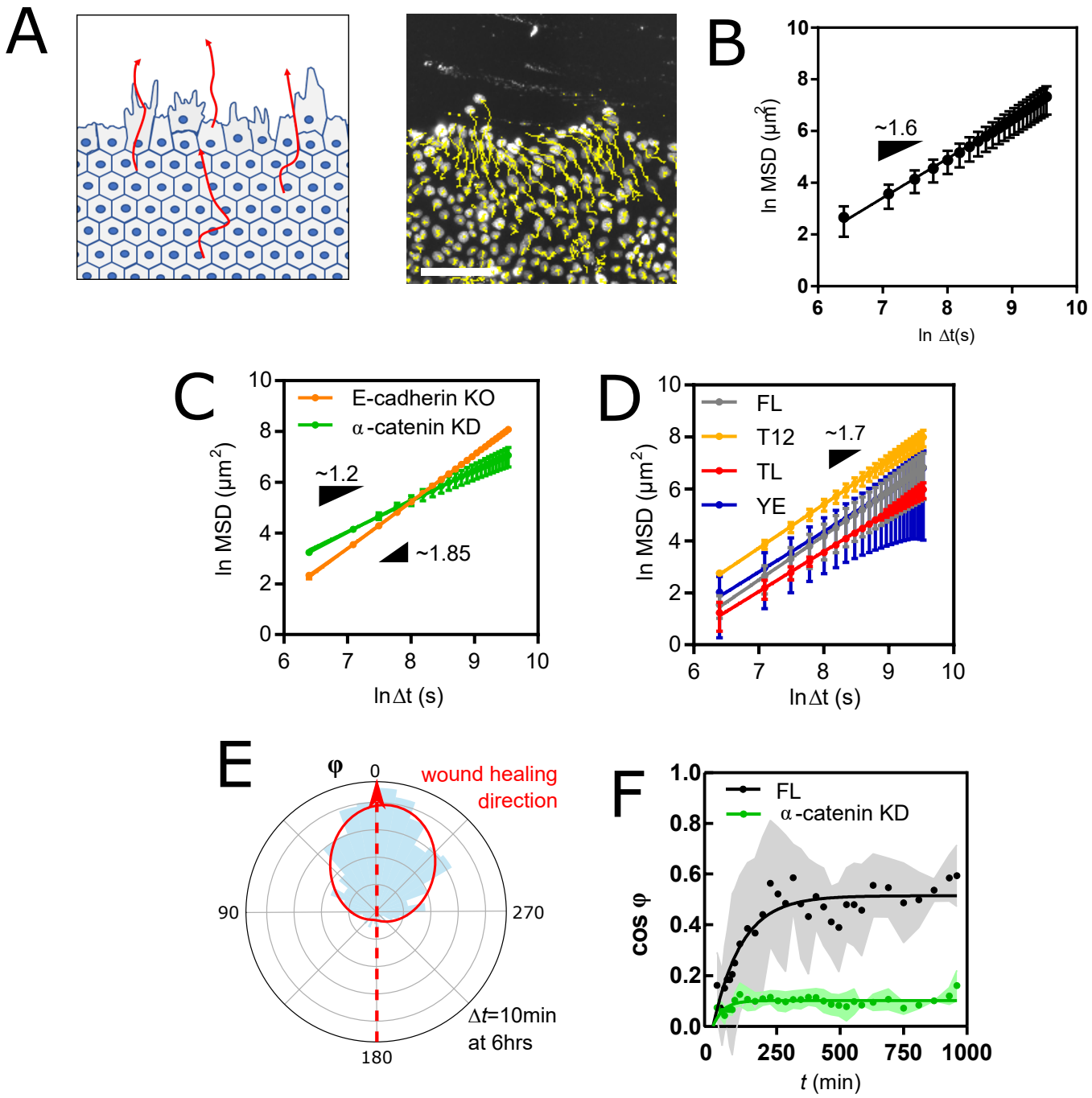

Fig. 5. (A) Left: Schematic representation of the guided collective cell migration assay. Right: fluorescence image of nucleus-stained cells and their migration tracks in yellow. Scale bar = 100μm. (B) MSD(Δt) of WT cells fit with a straight line in ln-ln scale. (C) MSD(Δt) of E-cadherin KO and α-catenin KD cells fit with a straight line in ln-ln scale. (D) MSD(Δt) of vinculin FL and mutant cells fit with a straight line in ln-ln scale. (E) Angular distribution of apparent velocities of vinculin FL cells at 6hrs post-wound fitted with a Von Mises distribution giving a concentration $\kappa \sim 1.3$ (solid red line). (F) Directionality ($\cos\phi(t)$, see Materials and Methods) of vinculin FL and α-catenin KD cells. All data from 4 (all but YE) and 3 (YE) FOV (500-1000 tracks each) of 4 (all but YE and α-catenin KD) and 3 (YE, α-catenin KD) independent experiments. Mean $\pm$ SEM.

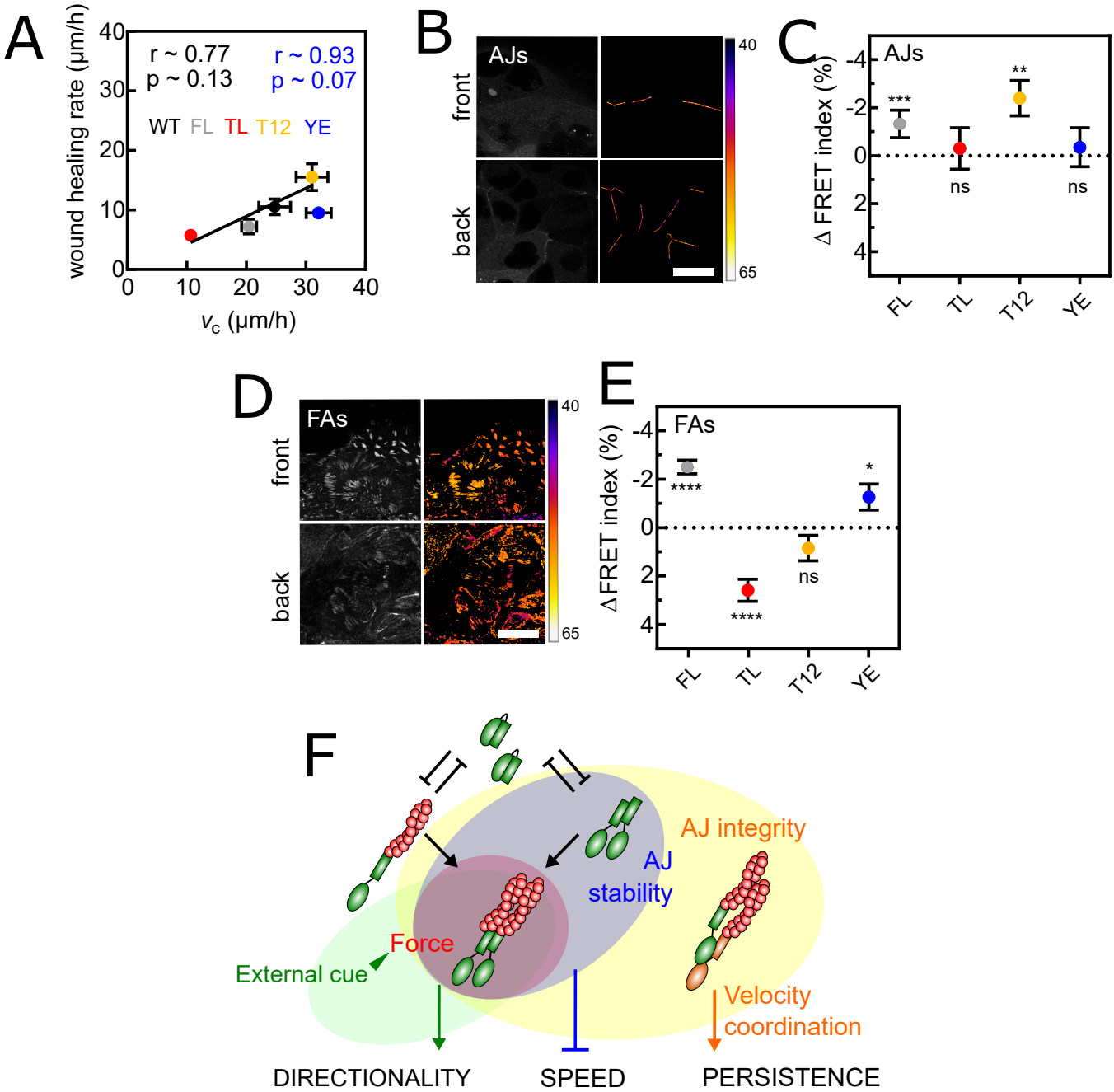

Fig. 6. (A) Wound healing rate (see Materials and Methods) as a function of cell speed at confluence for WT, vinculin FL and mutant cells. Pearson coefficients r and p-values in black for all data, in blue minus YE. (B) Left: direct fluorescence of vinculin TSMod in the AJs plane of cells at the wound front (top) and back (bottom). Right: corresponding FRET Index maps. (C) FRET Index difference between front and back cells at AJs of TSMod in vinculin FL and mutants. (D) Left: direct fluorescence of vinculin TSMod in the FAs plane of cells at the wound front (top) and back (bottom). Right: corresponding FRET Index maps. (E) FRET Index difference between front and back cells at FAs of TSMod in vinculin FL and mutants. (F) Proposed model: at AJs, vinculin dimerization and actin binding provide mechanosensitivity to stable AJs, which promotes wound healing. Data of (A) from 4 (all but YE) and 3 (YE) FOV of 4 (all but YE) and 3 (YE) independent experiments. Data of (C) from 55 (FL), 16 (TL), 56 (T12) and 26 (YE) front cells and 122 (FL), 30 (TL), 71 (T12) and 48 (YE) back cells of 4 (FL, T12) and 3 (TL, YE) independent experiments. Data of (E) from 144 (FL), 63 (TL), 124 (T12) and 46 (YE) front cells and 155 (FL), 84 (TL), 128 (T12) and 51 (YE) back cells of 7 (FL, T12), 4 (TL) and 3 (YE) independent experiments. Mean $\pm$ SEM. Two-tailed Mann-Whitney test between front and back cells for each construct (C,E). Scale bars = 50μm.

portional to their migration speed at confluence, YE mutant cells were less efficient in wound healing than expected (Fig. 6A). This supports that vinculin dimerization, in contrast to other vinculin tail interactions, promotes wound healing in a manner that cannot be explained from its effects on collective migration at confluence, nor on single cell migration.

To determine how such an effect might emerge from this mutant, we therefore excluded its impact on adhesion stability. Rather, we evaluated how vinculin tension perceived biased collective cell migration (Fig. 6B-E). Indeed, we had previously found that biased collective migration of epithelial cells imprints a transcellular gradient of molecular tension in E-cadherins, which are under higher tension away from the migration front (60). Consistently, we found that FL and T12 vinculin, both capable of dimerization and binding to actin, were increasingly recruited and under higher tension in AJs away from the migrating front (Fig. 6B, C). As expected, the TL mutant, incapable of dimerization or actin binding, did not show mechanosensitivity and, remarkably, neither did the YE mutant, only incapable of dimerization (Fig. 6C). Therefore, actin binding is not sufficient for vinculin to exhibit a transcellular tension gradient in AJs in response to a directional cue, dimerization is necessary.

In FAs (Fig. 6D, E), the TL mutant, which is insensitive to cytoskeletal tension by design, showed a lower FRET at the migration front. This suggests a cytoskeleton-independent increase in vinculin compression in back cells, as previously seen within single fibroblasts on adhesive patterns (61). The T12 mutant did not show a FRET gradient. Compared to TL, this suggests that an increase in cytoskeleton-dependent tension from front to back cells compensates for the opposite gradient of cytoskeleton-independent compression. FL vinculin showed a higher FRET at the migration fornt. This supports that the increase in tension from front to back cells overcompensates for the opposite gradient of cytoskeleton-independent compression. Remarkably, the YE mutant exhibited a mechanosensitivity similar to that of FL vinculin. This shows dimerization is not required for vinculin to exhibit a transcellular gradient in FAs in response to a directional cue.

Together, this shows that vinculin dimerization is involved in its mechanical sensitivity to external guidance cues only in AJs and not in FAs, while head-tail interaction is involved in none, and acting binding in both, expectedly. Overall, this supports that the wound healing rate scales with collective migration speed provided that both AJs and FAs are mechanosensitive to external guidance cues, a feature that depends on the dimerization of vinculin in AJs (Fig. 6F).

Discussion

In this work, we studied the exploratory capacity of epithelial cells, the influence of cell interactions and guidance cues on this exploration, and the dynamics and mechanics of the adhesion complexes that cells use in this process. Remarkably, we show that intercellular adhesion with neighbor cells within the epithelium provides virtually infinite directional memory for migration, as a result of velocity coordination. For this, proper interactions of AJs with the cytoskeleton through α-catenin are instrumental, but the type of cadherin involved is irrelevant. Additionally, cell speed depends on FAs stability and force transmission and is impeded by AJs stability, both controlled by vinculin. Finally, we show a specific role for vinculin dimerization in AJs, which regulates the mechanosensitivity of the epithelium as a whole to the guidance cue of a wound, and the wound healing rate of the epithelium.

Locomotion patterns of single cells have been observed and quantified for decades and can take many forms. When endowed with directional persistence arising from angular correlations between consecutive unit steps, cells adopt a so-called persistent random walk that eventually converges to a purely diffusive behavior, as initially observed in fibroblasts or single endothelial cells (4, 5). In contrast, in T cells and some metastatic cells that behave like Lévy walkers, the fat-tailed power-law distribution of step sizes results in superdiffusive behavior, even in the absence of temporal correlation in direction (7, 8). Here, our results show that single epithelial cells undergo a persistent random walk, with persistence on the order of several minutes to an hour depending on the cell line, beyond which cells diffuse purely (Fig. 1). Thus, the persistence of epithelial cells is in the low range compared to endothelial cells, whose persistence time can reach several hours (5). Furthermore, comparing cell lines that express various forms of vinculin mutants, we observe that persistence does not correlate with cell speed, consistent with endothelial cells exposed to growth factors (5). Mechanistically, both cell speed and persistence are under the control of actin retrograde flow, via connections with cell-matrix adhesions for the former, and control of polarity factors for the latter (62). Our data are thus consistent with the idea that the abnormal connection of cell-matrix adhesions to the cytoskeleton via vinculin uncouples speed from persistence.

Previously, vinculin-KO fibroblasts or epithelial cells have been shown to migrate faster than their WT counterparts (22, 24, 29). Here, we show that the migration speed of epithelial cells decreases with the expression of FL vinculin even at low levels above endogeneous (Fig. 1). Overall, this is consistent with the idea that vinculin acts primarily as a migration moderator, and this supports that insertion of the sensor module weakens to some extent the auto-inhibition of vinculin, thereby contributing to the dominance of all exogenous constructs over endogenous vinculin, in addition to the effects of their mutations. Mechanistically, our results support that the head-tail interaction of vinculin challenges both force transmission and stability of vinculin in FAs, as has been observed in other cell types (30, 44, 47–50), and is countered by the actin-vinculin tail interaction, which provides force transmission but is unnecessary for stability, and dimerization of the tail, which promotes stability and is dispensable for force transmission (Fig. 2D,E). Overall, the combination of maximum force transmission and stability predicts maximum cell speed (Fig. 2B). Therefore, we propose that the speed of single cells is the product of force transmission and stability in FAs (Fig. 2F, S5C).

At confluence, we show that epithelial cells adopt a superdiffusive behavior that a persistent random walk cannot explain (Fig. 2). This behavior has previously been observed in single cells or in a collective for a variety of cell types (6–8, 13–15). However, proposed models involved non-Gausian displacement distributions, which are sufficient to support superdiffusion without long-term memory. Moreover, whether superdiffusion in the collective emerged from intercellular interactions or from cells that already walk alone in this manner remained to be demonstrated. Here, we show that superdiffusion can be explained by a pure fractional Brownian motion with Gaussian distribution of displacement and virtually infinite directional memory, which emerges from intercellular interactions (Fig. 2A-D).

Previously, subdiffusive fractional Brownian motion has explained subcellular particle mobility in the crowded cytoplasm through interactions with the viscoelastic medium (63). In contrast, we show here that a strong superdiffusive fractional Brownian motion emerges from intercellular adhesion mediated by AJs bound to the cytoskeleton but independent of cadherin type, and not just steric hindrance due to the mere presence of neighboring cells (Fig. 3E,F). Remarkably, the same AJ-based mechanism also allows for velocity coordination between neighboring cells (Fig. S3E) (11). The interplay between persistent migration and elastic coupling provided by AJs was previously shown to be sufficient for velocity coordination (64). We further show with our minimal agent-based model that such coordination is sufficient to explain the transition to superdiffusion (Fig. 3G). Remarkably, the transition occurs in a region where $\alpha \sim 1.7$ for a number of interacting neighbors $n \sim 6$, about the number of direct neighbors at confluence, and $P_0/\tau \sim 3$. This allows us to determine the decision time τ, which is intrinsic to persistent random walks, but cannot be experimentally determined from single cell migration experiments that only reveal P_0. For MDCK cells with persistence $P_0 \sim 10$min, this corresponds to a decision time τ of a couple minutes. For RPE-1 cells with persistence $P_0 \sim 1$hr, τ would rather be several tens of minutes to an hour. This suggests that RPE-1 cells are more persistent due to their longer decision time, rather than narrower directional freedom. Discovering the respective molecular determinants of decision time and directional freedom appears as an exciting future research direction. In the same modeling context, others have shown that velocity coordination also results in spontaneous fluctuations in particle density (65). We thus propose that at confluence, such spatiotemporal fluctuations in the number of interacting neighbors generate variations in instantaneous persistence of cells along their trajectories, ultimately resulting in a distribution of persistence times across time scales. Consistently, the MSD of a persistent random walk at time P scales as P^{e-1}, the anomalous exponent being about that of the superdiffusive MSD, as if superdiffusing cells experienced a distribution of persistence times P that spanned all our experimentally accessible time scales.

In addition to inducing a transition from finite to infinite directional memory, we show that AJs have a second role: they globally decrease the apparent speed of cells, provided that vinculin is stable at AJs. Indeed, perturbation of vinculin dimerization leads to its low stability at AJs and faster than expected cell migration (Fig. 4B,F, S4C). Remarkably, this increase in cell speed is not the result of relaxed constraints on cortical deformations, as seen previously in unjamming transitions (66, 67), since vinculin mutants exhibit similar shapes indicative of a fluid phase (Fig. S4A). Alternatively, we speculate that the destabilization of AJs results in deeper intracellular changes within the cell's bulk, possibly due to the impaired ability to bundle actin of the vinculin mutant (43). This could therefore decrease the cell's own resistance to the bulk deformation required for migration but in a collective context only, and thus facilitate migration despite a less efficient FA machinery. Future studies may address this hypothesis.

Overall, intercellular adhesion normally impairs apparent cell speed but induces long-term directional persistence. As a result, while cells are collectively less efficient than single cells in exploring space at time scales of less than 3hrs, they can become more efficient beyond that (Fig. S3B). Thus, this emergence of long-term collective persistence may have a profound impact on tissue morphogenesis, regeneration, and homeostasis in a variety of contexts. In the case of wound healing, cells are further exposed to an external guidance cue. Here we show that this signal is sufficient to bias the velocity of each cell at the smallest experimental time scale (Fig. 5E). Detection of this signal is an emergent property of the collective, as disrupting intercellular adhesion renders cells nearly blind to the free space to invade (Fig. 5F). This is reminiscent of collective durotaxis and chemotaxis (68, 69). However, we show that this directional bias remains too small to drive ballistic motion in less than the longer experimental time range, such that cells remain superdiffusive throughout (Fig. 5A-D). We expect the directional bias to lead to more ballistic cell motion at longer time scales, with a lower limit of at least 3hrs.

This third role of AJs in directing collective cell migration is also dependent on vinculin. Specifically, wound healing rates scale with collective cell migtration speeds in a manner that depends on vinculin tail dimerization (Fig. 6A). In this context, vinculin tail dimerization is required to provide mechanosensitivity to AJs, so that both AJs and FAs can transmit molecular tension gradients across the tissue (Fig. 6B-E). This is again reminiscent of the requirements for supracellular durotaxis, which arises from intercellular force transmission (68). We speculate that the ability of cells to stiffen under force in a way that depends on vinculin dimerization may be involved (43).

In summary, we conclude that the spatial exploration efficiency of guided collective migration depends on the scale considered: at short time scales (<3hrs for MDCK cells), the intrinsic migration speed of individual cells is the limit, which can be overcome by collective directional memory at intermediate time scales (>3hrs for MDCK cells), a tissue-level property that guidance cues may additionally enhance, but at much longer time scales (»3hrs) (Fig. S5D). We

speculate that this generic framework applies qualitatively to guided collective migration in general and hope that future studies will test this prediction.

Materials and Methods

Live MDCK type II G cells stably expressing fluorescently tagged proteins were monitored on a wide-field epifluorescence inverted microscope for migration experiments, on a scanning spectral confocal microscope for FRET experiments, or on a spinning disk confocal microscope for FRAP experiments. Image analyses were performed with Imaris and ImageJ, simulations with R, data analyses with Matlab and R and statistics with Prism and R software. Complete materials and methods are available in Supplementary Materials and Methods. New materials, reagents, and simulation and analysis scripts are available upon request.

Data availability

This study does not include data deposited in external repositories.

ACKNOWLEDGEMENTS

We thank the members of the laboratory, C. Leclainche, S. Etienne-Manneville, B. Ladoux, P. Ronceray and R. Voituriez for insightful discussions. We thank C. Grashoff (Westfälische Wilhelms-Universität Münster), B. Ladoux and R.-M. Mège (Institut Jacques Monod), W. James Nelson (Stanford U.) and K. Schauer (Institut Gustave Roussy) for the gift of plasmids and cell lines. This work was supported in part by the Centre national de la recherche scientifique (CNRS), the French National Research Agency (ANR) grants (ANR-17-CE13-0013, ANR-17-CE09-0019, ANR-18-CE13-0008, ANR-21-CE13-0048), the Investments for the Future program of the French Government (LabEx Who am I? ANR-11-LABX-0071, Université Paris Cité ANR-18-IDEX-0001) and the Association pour la Recherche contre le Cancer (ARC-PJA22020060002255). We acknowledge the ImagoSeine facility, member of the France BioImaging infrastructure (ANR-10-INSB-04), and the Institut Jacques Monod IT team. HC was supported by La Ligue contre le Cancer (TAYS18872) and Fondation Recherche Médicale (FDT202001010843).

References

1. Peter Friedl and Darren Gilmour. Collective cell migration in morphogenesis, regeneration and cancer. *Nature Reviews Molecular Cell Biology 2009 10:7*, 10(7):445–457, jul 2009. ISSN 1471-0080. doi: 10.1038/NRM2720.
2. Peter Friedl and Katarina Wolf. Plasticity of cell migration: a multiscale tuning model. *The Journal of cell biology*, 188(1):11–19, 2010. doi: 10.1083/jcb.200909003.
3. M Abercrombie and Joan E M Heaysman. Observations on the social behaviour of cells in tissue culture : I. Speed of movement of chick heart fibroblasts in relation to their mutual contacts. *Experimental Cell Research*, 5(1):111–131, 1953.
4. Mitchell H. Gail and Charles W. Boone. The Locomotion of Mouse Fibroblasts in Tissue Culture. *Biophysical Journal*, 10(10):980–993, oct 1970. ISSN 00063495. doi: 10.1016/S0006-3495(70)86347-0.
5. C.L. Stokes, D.A. Lauffenburger, and S.K. Williams. Migration of individual microvessel endothelial cells: stochastic model and parameter measurement. *Journal of Cell Science*, 99(2), 1991.
6. Peter Dieterich, Rainer Klages, Roland Preuss, and Albrecht Schwab. Anomalous dynamics of cell migration. *Proceedings of the National Academy of Sciences of the United States of America*, 105(2):459–463, jan 2008. ISSN 00278424. doi: 10.1073/pnas.0707603105.
7. Tajie H. Harris, Edward J. Banigan, David A. Christian, Christoph Konradt, Elia D.Tait Wojno, Kazumi Norose, Emma H. Wilson, Beena John, Wolfgang Weninger, Andrew D. Luster, Andrea J. Liu, and Christopher A. Hunter. Generalized Lévy walks and the role of chemokines in migration of effector CD8 + T cells. *Nature*, 486(7404):545–548, jun 2012. ISSN 00280836. doi: 10.1038/nature11098.
8. Sabil Huda, Bettina Weigelin, Katarina Wolf, Konstantin V. Tretiakov, Konstantin Polev, Gary Wilk, Masatomo Iwasa, Fateme S. Emami, Jakub W. Narojczyk, Michal Banaszak, Siowling Soh, Didzis Pilans, Amir Vahid, Monika Makurath, Peter Friedl, Gary G. Borisy, Kristiana Kandere-Grzybowska, and Bartosz A. Grzybowski. Lévy-like movement patterns of metastatic cancer cells revealed in microfabricated systems and implicated in vivo. *Nature Communications*, 9(1):1–11, dec 2018. ISSN 20411723. doi: 10.1038/s41467-018-06563-w.
9. B. Szabó, G. J. Szöllösi, B. Gönci, Zs Jurányi, D. Selmeczi, and Tamás Vicsek. Phase transition in the collective migration of tissue cells: Experiment and model. *Physical Review E - Statistical, Nonlinear, and Soft Matter Physics*, 74(6):061908, dec 2006. ISSN 15393755. doi: 10.1103/PHYSREVE.74.061908/FIGURES/5/MEDIUM.
10. Philip Vitorino, Mark Hammer, Jongmin Kim, and Tobias Meyer. A Steering Model of Endothelial Sheet Migration Recapitulates Monolayer Integrity and Directed Collective Migration. *Molecular and Cellular Biology*, 31(2):342–350, jan 2011. doi: 10.1128/MCB.00800-10.
11. N. Borghi, M. Lowndes, V. Maruthamuthu, M.L. Gardel, and W.J. Nelson. Regulation of cell motile behavior by crosstalk between cadherin- and integrin-mediated adhesions. *Proceedings of the National Academy of Sciences of the United States of America*, 107(30), 2010. ISSN 10916490. doi: 10.1073/pnas.1002662107.
12. Adam Shellard and Roberto Mayor. Rules of collective migration: From the wildebeest to the neural crest: Rules of neural crest migration. *Philosophical Transactions of the Royal Society B: Biological Sciences*, 375(1807), sep 2020. ISSN 14712970. doi: 10.1098/rstb.2019.0387.
13. Hisashi Haga, Chikako Irahara, Ryo Kobayashi, Toshiyuki Nakagaki, and Kazushige Kawabata. Collective Movement of Epithelial Cells on a Collagen Gel Substrate. *Biophysical Journal*, 88(3):2250–2256, mar 2005.
14. Kenechukwu David Nnetu, Melanie Knorr, Steve Pawlizak, Thomas Fuhs, and Josef A. Käs. Slow and anomalous dynamics of an MCF-10A epithelial cell monolayer. *Soft Matter*, 9(39): 9335–9341, sep 2013. ISSN 1744-6848. doi: 10.1039/C3SM50806D.
15. Tatiane Souza Vilela Podestá, Tiago Venzel Rosembach, Anésia Aparecida Dos Santos, and Marcelo Lobato Martins. Anomalous diffusion and q-Weibull velocity distributions in epithelial cell migration. *PLoS ONE*, 12(7), jul 2017. ISSN 19326203. doi: 10.1371/journal.pone.0180777.
16. Michael P. Sheetz, Dan P. Felsenfeld, and Catherine G. Galbraith. Cell migration: regulation of force on extracellular-matrix-integrin complexes. *Trends in cell biology*, 8(2):51–54, 1998. ISSN 0962-8924. doi: 10.1016/S0962-8924(98)80005-6.
17. Nathalie Q Balaban, Ulrich S Schwarz, Daniel Riveline, Polina Goichberg, Gila Tzur, Ilana Sabanay, Diana Mahalu, Sam Safran, Alexander Bershadsky, Lia Addadi, and Benjamin Geiger. Force and focal adhesion assembly: a close relationship studied using elastic micropatterned substrates. *Nat Cell Biol*, 3(5):466–472, may 2001. ISSN 1465-7392.
18. Shigenobu Yonemura, Yuko Wada, Toshiyuki Watanabe, Akira Nagafuchi, and Mai Shibata. Alpha-Catenin as a tension transducer that induces adherens junction development. *Nature cell biology*, 12(6):533–542, 2010. ISSN 1465-7392. doi: 10.1038/ncb2055.
19. Robert P. Johnson and Susan W. Craig. Actin Activates a Cryptic Dimerization Potential of the Vinculin Tail Domain. *Journal of Biological Chemistry*, 275(1):95–105, jan 2000. ISSN 0021-9258. doi: 10.1074/JBC.275.1.95.
20. Mitsuko Watabe-Uchida, Naoshige Uchida, Yuzo Imamura, Akira Nagafuchi, Kazushi Fujimoto, Tadashi Uemura, Stefan Vermeulen, Frans van Roy, Eileen D Adamson, and Masatoshi Takeichi. alpha -Catenin-Vinculin Interaction Functions to Organize the Apical Junctional Complex in Epithelial Cells. *The Journal of Cell Biology*, 142(3):847–857, aug 1998.
21. Karry M Jannie, Shawn M Ellerbroek, Dennis W Zhou, Sophia Chen, David J Crompton, Andrés J García, and Kris A DeMali. Vinculin-dependent actin bundling regulates cell migration and traction forces. *The Biochemical journal*, 465(3):383–93, feb 2015. ISSN 1470-8728. doi: 10.1042/BJ20140872.
22. Hyunna T. Lee, Lisa Sharek, E. Timothy O'Brien, Fabio L. Urbina, Stephanie L. Gupton, Richard Superfine, Keith Burridge, and Sharon L. Campbell. Vinculin and metavinculin exhibit distinct effects on focal adhesion properties, cell migration, and mechanotransduction. *PLOS ONE*, 14(9):e0221962, sep 2019. ISSN 1932-6203. doi: 10.1371/journal.pone.0221962.
23. M Cecilia Subauste, Olivier Pertz, Eileen D Adamson, Christopher E Turner, Sachiko Junger, and Klaus M Hahn. Vinculin modulation of paxillin-FAK interactions regulates ERK to control survival and motility. *The Journal of cell biology*, 165(3):371–81, may 2004. ISSN 0021-9525. doi: 10.1083/jcb.200308011.
24. W Xu, JL Coll, and ED Adamson. Rescue of the mutant phenotype by reexpression of full-length vinculin in null F9 cells; effects on cell locomotion by domain deleted vinculin. *J. Cell Sci.*, 111(11):1535–1544, jun 1998.
25. Aniqua Rahman, Shawn P. Carey, Casey M. Kraning-Rush, Zachary E. Goldblatt, Francois Bordeleau, Marsha C. Lampi, Deanna Y. Lin, Andrés J. García, and Cynthia A. Reinhart-King. Vinculin regulates directionality and cell polarity in two-And three-dimensional matrix and three-dimensional microtrack migration. *Molecular Biology of the Cell*, 27(9):1431–1441, may 2016. ISSN 19394586. doi: 10.1091/MBC.E15-06-0432/ASSET/IMAGES/LARGE/MBC-27-1431-G007.JPEG.
26. J. R. Carvalho, I. C. Fortunato, C. G. Fonseca, A. Pezzarossa, P. Barbacena, M. A. Dominguez-Cejudo, F. F. Vasconcelos, N. C. Santos, F. A. Carvalho, and Claudio A. Franco. Non-canonical Wnt signaling regulates junctional mechanocoupling during angiogenic collective cell migration. *eLife*, 8, jun 2019. ISSN 2050084X. doi: 10.7554/eLife.45853.001.
27. Jianzhong Ai, Tao Jin, Lu Yang, Qiang Wei, Yang Yang, Hong Li, Ye Zhu, Jianzhong Ai, Tao Jin, Lu Yang, Qiang Wei, Yang Yang, Hong Li, and Ye Zhu. Vinculin and filamin-C are two potential prognostic biomarkers and therapeutic targets for prostate cancer cell migration. *Oncotarget*, 8(47):82430–82436, jul 2017. ISSN 1949-2553. doi: 10.18632/ONCOTARGET.19397.
28. Stefan Moese, Matthias Selbach, Volker Brinkmann, Alexander Karlas, Beatrice Haimovich, Steffen Backert, and Thomas F. Meyer. The Helicobacter pylori CagA protein disrupts matrix adhesion of gastric epithelial cells by dephosphorylation of vinculin. *Cellular Microbiology*, 9(5):1148–1161, may 2007. ISSN 1462-5822. doi: 10.1111/J.1462-5822.2006.00856.X.
29. J. L. Coll, A. Ben-Ze'ev, R. M. Ezzell, J. L. Rodríguez Fernández, H. Baribault, R. G. Oshima, and E. D. Adamson. Targeted disruption of vinculin genes in F9 and embryonic stem cells changes cell morphology, adhesion, and locomotion. *Proceedings of the National Academy of Sciences of the United States of America*, 92(20):9161–9165, sep 1995. ISSN 00278424. doi: 10.1073/pnas.92.20.9161.
30. Alex Carisey, Ricky Tsang, Alexandra M Greiner, Nadja Nijenhuis, Nikki Heath, Alicja Nazgiewicz, Ralf Kemkemer, Brian Derby, Joachim Spatz, and Christoph Ballestrem. Vinculin regulates the recruitment and release of core focal adhesion proteins in a force-dependent manner. *Current Biology*, 23(4):271–81, feb 2013. ISSN 1879-0445. doi: 10.1016/j.cub.2013.01.009.
31. Jennifer L Bays, Xiao Peng, Catlin E Tolbert, Christophe Guilluy, Ashley E Angell, Yuan Pan, Richard Superfine, Keith Burridge, and Kris A DeMali. Vinculin phosphorylation differentially

regulates mechanotransduction at cell-cell and cell-matrix adhesions. *The Journal of cell biology*, 205(2):251–63, apr 2014. ISSN 1540-8140. doi: 10.1083/jcb.201309092.

32. Katheryn E. Rothenberg, David W. Scott, Nicolas Christoforou, and Brenton D. Hoffman. Vinculin Force-Sensitive Dynamics at Focal Adhesions Enable Effective Directed Cell Migration. *Biophysical Journal*, 114(7):1680–1694, apr 2018. ISSN 0006-3495. doi: 10.1016/J.BPJ.2018.02.019.
33. Jacqueline M Benjamin, Adam V Kwiatkowski, Changsong Yang, Farida Korobova, Sabine Pokutta, Tatyana Svitkina, William I Weis, and W James Nelson. Alpha-E-catenin regulates actin dynamics independently of cadherin-mediated cell–cell adhesion. *Journal Of Cell Biology*, 189(2):339–352, 2010. doi: 10.1083/jcb.200910041.
34. Rima Seddiki, Gautham Hari Narayana Sankara Narayana, Pierre-Olivier Strale, Hayri Emrah Balcioglu, Grégoire Peyret, Mingxi Yao, Anh Phuong Le, Chwee Teck Lim, Jie Yan, Benoit Ladoux, and René Marc Mège. Force-dependent binding of vinculin to α-catenin regulates cell-cell contact stability and collective cell behavior. *Molecular biology of the cell*, 29(4):380–388, feb 2018. ISSN 1939-4586. doi: 10.1091/mbc.E17-04-0231.
35. Joseph Candiello, Manimalha Balasubramani, Emmanuel M. Schreiber, Gregory J. Cole, Ulrike Mayer, Willi Halfter, and Hai Lin. Biomechanical properties of native basement membranes. *FEBS Journal*, 274(11):2897–2908, June 2007. ISSN 1742464X. doi: 10.1111/j.1742-4658.2007.05823.x. Publisher: Blackwell Publishing Ltd.
36. Larry W. Welling and Jared J. Grantham. Physical properties of isolated perfused renal tubules and tubular basement membranes. *Journal of Clinical Investigation*, 51(5):1063–1075, May 1972. ISSN 0021-9738. doi: 10.1172/JCI106898.
37. R. F. Fisher. The influence of age on some ocular basement membranes. *Eye*, 1(2):184–189, March 1987. ISSN 1476-5454. doi: 10.1038/eye.1987.35. Publisher: Nature Publishing Group.
38. Reinholdrth Fürth. Die Brownsche Bewegung bei Berücksichtigung einer Persistenz der Bewegungsrichtung. Mit Anwendungen auf die Bewegung lebender Infusorien. *Zeitschrift für Physik*, 2(3):244–256, jun 1920. ISSN 14346001. doi: 10.1007/BF01328731.
39. G. E. Uhlenbeck and L. S. Ornstein. On the theory of the Brownian motion. *Physical Review*, 36(5):823–841, sep 1930. ISSN 0031899X. doi: 10.1103/PhysRev.36.823.
40. Carsten Grashoff, B.D. Hoffman, M.D. Brenner, Ruobo Zhou, Maddy Parsons, M.T. Yang, M.A. McLean, S.G. Sligar, C.S. Chen, Taekjip Ha, and Others. Measuring mechanical tension across vinculin reveals regulation of focal adhesion dynamics. *Nature*, 466(7303): 263–266, 2010. doi: 10.1038/nature09198.
41. Matthew G Rubashkin, Luke Cassereau, Russell Bainer, Christopher C DuFort, Yoshihiro Yui, Guanqing Ou, Matthew J Paszek, Michael W Davidson, Yunn-Yi Chen, and Valerie M Weaver. Force engages vinculin and promotes tumor progression by enhancing PI3K activation of phosphatidylinositol (3,4,5)-triphosphate. *Cancer research*, 74(17):4597–611, sep 2014. ISSN 1538-7445. doi: 10.1158/0008-5472.CAN-13-3698.
42. Daniel M Cohen, Hui Chen, Robert P Johnson, Begum Choudhury, and Susan W Craig. Two distinct head-tail interfaces cooperate to suppress activation of vinculin by talin. *The Journal of biological chemistry*, 280(17):17109–17, apr 2005. ISSN 0021-9258. doi: 10.1074/jbc.M414704200.
43. Caitlin E. Tolbert, Peter M. Thompson, Richard Superfine, Keith Burridge, and Sharon L. Campbell. Phosphorylation at Y1065 in Vinculin Mediates Actin Bundling, Cell Spreading, and Mechanical Responses to Force. *Biochemistry*, 53(34):5526–5536, sep 2014. ISSN 0006-2960. doi: 10.1021/bi500678x.
44. Jonathan D Humphries, Pengbo Wang, Charles Streuli, Benny Geiger, Martin J Humphries, and Christoph Ballestrem. Vinculin controls focal adhesion formation by direct interactions with talin and actin. *The Journal of Cell Biology*, 179(5):1043–1057, dec 2007.
45. Katharina Austen, Pia Ringer, Alexander Mehlich, Anna Chrostek-Grashoff, Carleen Kluger, Christoph Klingner, Benedikt Sabass, Roy Zent, Matthias Rief, and Carsten Grashoff. Extracellular rigidity sensing by talin isoform-specific mechanical linkages. *Nature cell biology*, nov 2015. ISSN 1476-4679. doi: 10.1038/ncb3268.
46. Pia Ringer, Andreas Weißl, Anna-Lena Cost, Andrea Freikamp, Benedikt Sabass, Alexander Mehlich, Marc Tramier, Matthias Rief, and Carsten Grashoff. Multiplexing molecular tension sensors reveals piconewton force gradient across talin-1. *Nature Methods*, 14(11): 1090–1096, sep 2017. ISSN 1548-7091. doi: 10.1038/nmeth.4431.
47. Zengzhen Liu, Philippe Bun, Nicolas Audugé, Maïté Coppey-Moisan, and Nicolas Borghi. Vinculin head-tail interaction defines multiple early mechanisms for cell substrate rigidity sensing. *Integrative biology*, 8(6):693–703, may 2016. ISSN 1757-9708. doi: 10.1039/c5ib00307e.
48. Daniel M Cohen, Brett Kutscher, Hui Chen, Douglas B Murphy, and Susan W Craig. A Conformational Switch in Vinculin Drives Formation and Dynamics of a Talin-Vinculin Complex at Focal Adhesions. *Journal of Biological Chemistry*, 281(23):16006–16015, jun 2006.
49. D. W. Dumbauld, T. T. Lee, A. Singh, J. Scrimgeour, C. A. Gersbach, E. A. Zamir, J. Fu, C. S. Chen, J. E. Curtis, S. W. Craig, and A. J. Garcia. How vinculin regulates force transmission. *Proceedings of the National Academy of Sciences*, 110(24):9788–9793, may 2013. ISSN 0027-8424. doi: 10.1073/pnas.1216209110.
50. Tomohiro Omachi, Takafumi Ichikawa, Yasuhisa Kimura, Kazumitsu Ueda, and Noriyuki Kioka. Vinculin association with actin cytoskeleton is necessary for stiffness-dependent regulation of vinculin behavior. *PLOS ONE*, 12(4):e0175324, apr 2017. ISSN 1932-6203. doi: 10.1371/journal.pone.0175324.
51. Dapeng Bi, J. H. Lopez, J. M. Schwarz, and M. Lisa Manning. A density-independent rigidity transition in biological tissues. *Nature Physics*, 11(12):1074–1079, dec 2015. ISSN 1745-2473. doi: 10.1038/nphys3471.
52. Benoit B. Mandelbrot and John W. Van Ness. Fractional Brownian Motions, Fractional Noises and Applications. *SIAM Review*, 10(4):422–437, oct 1968. ISSN 0036-1445. doi: 10.1137/1010093.
53. Christopher T Capaldo and Ian G Macara. Depletion of E-Cadherin Disrupts Establishment but Not Maintenance of Cell Junctions in Madin-Darby Canine Kidney Epithelial Cells. *Molecular Biology of the Cell*, 18(1):189–200, jan 2007.
54. Christopher L Tinkle, H Amalia Pasolli, Nicole Stokes, and Elaine Fuchs. New insights into cadherin function in epidermal sheet formation and maintenance of tissue integrity. *Proceedings of the National Academy of Sciences*, 105(40):15405–15410, oct 2008.
55. Judith A. Tunggal, Iris Helfrich, Annika Schmitz, Heinz Schwarz, Dorothee Günzel, Michael Fromm, Rolf Kemler, Thomas Krieg, and Carien M. Niessen. E-cadherin is essential for in vivo epidermal barrier function by regulating tight junctions. *The EMBO Journal*, 24(6): 1146–1156, mar 2005. ISSN 1460-2075. doi: 10.1038/SJ.EMBOJ.7600605.
56. Elsa Bazellières, Vito Conte, Alberto Elosegui-Artola, Xavier Serra-Picamal, María Bintanel-Morcillo, Pere Roca-Cusachs, José J. Muñoz, Marta Sales-Pardo, Roger Guimerà, and Xavier Trepat. Control of cell–cell forces and collective cell dynamics by the intercellular adhesome. *Nature Cell Biology*, 17(4):409–420, apr 2015. ISSN 1465-7392. doi: 10.1038/ncb3135.
57. Tams Vicsek, Andrs Czirk, Eshel Ben-Jacob, Inon Cohen, and Ofer Shochet. Novel type of phase transition in a system of self-driven particles. *Physical Review Letters*, 75(6):1226–1229, aug 1995. ISSN 00319007. doi: 10.1103/PhysRevLett.75.1226.
58. Joanne M Leerberg, Guillermo A Gomez, Suzie Verma, Elliott J Moussa, Selwin K Wu, Rashmi Priya, Brenton D Hoffman, Carsten Grashoff, Martin A Schwartz, and Alpha S Yap. Tension-Sensitive Actin Assembly Supports Contractility at the Epithelial Zonula Adherens. *Current biology : CB*, jul 2014. ISSN 1879-0445. doi: 10.1016/j.cub.2014.06.028.
59. L. Petitjean, M. Reffay, E. Grasland-Mongrain, M. Poujade, B. Ladoux, A. Buguin, and P. Silberzan. Velocity Fields in a Collectively Migrating Epithelium. *Biophysical Journal*, 98(9): 1790–1800, may 2010. doi: 10.1016/j.bpj.2010.01.030.
60. Charlène Gayrard, Clément Bernaudin, Théophile Déjardin, Cynthia Seiler, and Nicolas Borghi. Src- and confinement-dependent FAK activation causes E-cadherin relaxation and β-catenin activity. *The Journal of cell biology*, 217(3):1063–1077, mar 2018. ISSN 1540-8140. doi: 10.1083/jcb.201706013.
61. Katheryn E. Rothenberg, Shane S. Neibart, Andrew S. LaCroix, and Brenton D. Hoffman. Controlling Cell Geometry Affects the Spatial Distribution of Load Across Vinculin. *Cellular and Molecular Bioengineering*, 8(3):364–382, sep 2015. ISSN 1865-5025. doi: 10.1007/s12195-015-0404-9.
62. Paolo Maiuri, Jean-François Rupprecht, Stefan Wieser, Verena Ruprecht, Olivier Bénichou, Nicolas Carpi, Mathieu Coppey, Simon De Beco, Nir Gov, Carl-Philipp Heisenberg, Carolina Lage Crespo, Franziska Lautenschlaeger, Maël Le Berre, Ana-Maria Lennon-Dumenil, Matthew Raab, Hawa-Racine Thiam, Matthieu Piel, Michael Sixt, and Raphaël Voituriez. Actin flows mediate a universal coupling between cell speed and cell persistence. *Cell*, 161 (2):374–86, apr 2015. ISSN 1097-4172. doi: 10.1016/j.cell.2015.01.056.
63. Yasmine Meroz and Igor M. Sokolov. A toolbox for determining subdiffusive mechanisms. *Physics Reports*, 573:1–29, apr 2015. ISSN 03701573. doi: 10.1016/j.physrep.2015.01.002.
64. Silke Henkes, Kaja Kostanjevec, J. Martin Collinson, Rastko Sknepnek, and Eric Bertin. Dense active matter model of motion patterns in confluent cell monolayers. *Nature Communications 2020 11:1*, 11(1):1–9, mar 2020. ISSN 2041-1723. doi: 10.1038/s41467-020-15164-5.
65. Hugues Chaté, Francesco Ginelli, Guillaume Grégoire, and Franck Raynaud. Collective motion of self-propelled particles interacting without cohesion. *Physical Review E - Statistical, Nonlinear, and Soft Matter Physics*, 77(4):046113, apr 2008. ISSN 15393755. doi: 10.1103/PHYSREVE.77.046113/FIGURES/21/MEDIUM.
66. Jin Ah Park, Jae Hun Kim, Dapeng Bi, Jennifer A. Mitchel, Nader Taheri Qazvini, Kelan Tantisira, Chan Young Park, Maureen McGill, Sae Hoon Kim, Bomi Gweon, Jacob Notbohm, Robert Steward, Stephanie Burger, Scott H. Randell, Alvin T. Kho, Dhananjay T. Tambe, Corey Hardin, Stephanie A. Shore, Elliot Israel, David A. Weitz, Daniel J. Tschumperlin, Elizabeth P. Henske, Scott T. Weiss, M. Lisa Manning, James P. Butler, Jeffrey M. Drazen, and Jeffrey J. Fredberg. Unjamming and cell shape in the asthmatic airway epithelium. *Nature Materials*, 14(10):1040–1048, oct 2015. ISSN 14764660. doi: 10.1038/nmat4357.
67. Chiara Malinverno, Salvatore Corallino, Fabio Giavazzi, Martin Bergert, Qingsen Li, Marco Leoni, Andrea Disanza, Emanuela Frittoli, Amanda Oldani, Emanuele Martini, Tobias Lendenmann, Gianluca Deflorian, Galina V. Beznoussenko, Dimos Poulikakos, Kok Haur Ong, Marina Uroz, Xavier Trepat, Dario Parazzoli, Paolo Maiuri, Weimiao Yu, Aldo Ferrari, Roberto Cerbino, and Giorgio Scita. Endocytic reawakening of motility in jammed epithelia. *Nature Materials*, 16(5):587–596, may 2017. ISSN 14764660. doi: 10.1038/nmat4848.
68. Raimon Sunyer, Vito Conte, Jorge Escribano, Alberto Elosegui-Artola, Anna Labernadie, Léo Valon, Daniel Navajas, José Manuel García-Aznar, José J Muñoz, Pere Roca-Cusachs, and Xavier Trepat. Collective cell durotaxis emerges from long-range intercellular force transmission. *Science (New York, N.Y.)*, 353(6304):1157–61, sep 2016. ISSN 1095-9203. doi: 10.1126/science.aaf7119.
69. Eric Theveneau, Lorena Marchant, Sei Kuriyama, Mazhar Gull, Barbara Moepps, Maddy Parsons, and Roberto Mayor. Collective Chemotaxis Requires Contact-Dependent Cell Polarity. *Developmental Cell*, 19(1):39–53, jul 2010. ISSN 1534-5807. doi: 10.1016/J.DEVCEL.2010.06.012.